



OPEN UW supplementation with AP39 improves liver viability following static cold storage

McLean Taggart^{1,2}, Saige Holkup¹, Alexandra Tchir^{1,2,3}, Mohammadreza Mojoudi^{1,2}, Arnaud Lyon^{1,2}, Madeeha Hassan^{1,2}, Christopher Taveras^{1,2}, Ozge Sila Ozgur^{1,2}, James F. Markmann⁴, Heidi Yeh^{1,5}, Korkut Uygun^{1,2,6}✉ & Alban Longchamp^{1,2,5,6}✉

Static cold storage of donor livers at 4 °C incompletely arrests metabolism, ultimately leading to decreases in ATP levels, oxidative stress, cell death, and organ failure. Hydrogen Sulfide (H₂S) is an endogenously produced gas, previously demonstrated to reduce oxidative stress, reduce ATP depletion, and protect from ischemia and reperfusion injury. H₂S is difficult to administer due to its rapid release curve, resulting in cellular death at high concentrations. AP39, a mitochondrially targeted, slow-release H₂S donor, has been shown to reduce ischemia-reperfusion injury in hearts and kidneys. Thus, we investigated whether the addition of AP39 during 3-day static cold storage can improve liver graft viability. At the end of storage, livers underwent six hours of acellular normothermic machine perfusion, a model of transplantation. During simulated transplantation, livers stored with AP39 showed reduced resistance, reduced cellular damage (ALT and AST), and reduced apoptosis. Additionally, bile production and glucose, as well as energy charge were improved by the addition of AP39. These results indicate that AP39 supplementation improves liver viability during static cold storage.

Liver transplantation is the only viable treatment option for patients in end-stage liver failure. However, its broad application is limited by the number of available donor organs¹. A significant limiting factor to the expansion of the donor pool is the loss of viability occurring during transport/preservation. The duration of ischemic cold storage correlates with early allograft dysfunction (EAD) and reduced long-term survival of the grafts². As a result, thousands of organs are discarded each year³. This clinical problem suggests that better preservation techniques are needed to improve graft quality and help combat the global donor organ shortage crisis⁴.

Hydrogen sulfide (H₂S) is an endogenously produced gaseous molecule through both enzymatic degradation of cysteine via cystathionine γ -lyase (CGL), or non-enzymatic degradation of thiol-containing molecules⁵. H₂S is proangiogenic, reduces mitochondrial stress, and can regulate the eNOS-NO pathway^{6,7}. H₂S also has anti-inflammatory and antioxidant properties, and can reversibly inhibit the mitochondrial electron transport chain, thus reducing reactive oxygen species (ROS) formation during reperfusion⁸. During ischemia, H₂S promotes glucose uptake and glycolytic ATP production⁹. Mice lacking endogenous H₂S production showed increased damage and mortality following renal ischemia-reperfusion injury, and the introduction of exogenous H₂S (NaHS) was shown to reverse this effect¹⁰. Similarly, it has been shown that the introduction of exogenous NaHS in wild-type mice reduces both hepatic and renal ischemia-reperfusion injury^{10,11}. The addition of NaHS to University of Wisconsin solution (UW) preservation solution during SCS reduced necrosis and apoptosis, improving kidney function after transplantation in rats¹². Despite great success in mitigating the effect of ischemia, NaHS is limited in its application due to the rapid, uncontrollable rate of H₂S production, resulting in inhibition of mitochondrial electron complexes I and IV and cellular death at high concentrations^{13,14}.

AP39 is a mitochondrial-targeting, slow-release H₂S donor synthesized to improve the mito-protective effects of H₂S via extended release, and sustained, low-dose release for up to 10 days. Additionally, the introduction of a TPP moiety^{15,16} targets H₂S at the mitochondria. In a rat kidney transplant model, SCS with 200 nM AP39, resulted in approximately three times increase in survival at 7 days, and increased creatinine clearance¹⁷. Consistently, the addition of AP39 during porcine kidneys subnormothermic perfusion (21 °C) for 4 h with an O₂ carrier (Hemopure) improved urine output and graft oxygenation¹⁸. In renal epithelial cells, the addition of

¹Center for Engineering in Medicine and Surgery, Massachusetts General Hospital, Harvard Medical School, Boston, MA, USA. ²Shriners Children's Boston, Boston, MA, USA. ³Massachusetts Institute of Technology, Boston, MA, USA.

⁴Penn Transplant Institute, University of Pennsylvania, Philadelphia, PA, USA. ⁵Center for Transplantation Sciences, Massachusetts General Hospital, Boston, MA, USA. ⁶Korkut Uygun and Alban Longchamp contributed equally to this work. ✉email: KUYGUN@mgh.harvard.edu; alongchamp@mgh.harvard.edu

400 nM AP39 during SCS reduced ROS production¹⁷. Similarly, in a heterotopic mouse heart transplant model, 200 nM AP39 improved left ventricular ejection fraction and reduced fibrosis following transplantation 24 h after SCS¹⁹.

In the liver, hepatocytes, make up 20–25% of overall cellular volume. Mitochondria are the main energy source in hepatocytes and are at the center of many of the signaling pathways that mediate hepatocyte injury during ischemia. Thus, we hypothesized that AP39 supplementation could improve liver viability during SCS. In this study, we tested the benefits of AP39 during liver SCS for 3 days. This storage period was chosen based on previous studies showing 100% transplantability after 24 h of SCS, and 50% following 48 h; using a storage period just beyond transplantability enabled sufficient injury following acellular normothermic reperfusion^{20,21}. Following storage, liver viability was evaluated using acellular machine perfusion, allowing real-time assessment of perfusion quality and molecular injury (Fig. 1).

Methods

Liver procurement

This study is reported in accordance with ARRIVE guidelines. Female Lewis rats (250–300 g, Charles River Laboratories, Boston MA, USA) were socially housed in controlled, standard conditions (12-hour light/day cycle, 12C, 30–70% humidity, pathogen-free HEPA filtered ventilated cages, mixed paper/cellulose bedding). All rats had unfettered access to sterile water and chow, as in accordance with National Research Council Guidelines. All rats were cared for by the Massachusetts General Hospital (MGH) Center for Comparative Medicine (CCM). The experimental protocol was approved by the Institutional Care and Use Committee (IACUC) of MGH (Protocol #2011N000111), and all experiments were performed in accordance with established guidelines. Livers were procured as previously described²². Briefly, donor rats were anesthetized under 3% isoflurane and maintained at 1%. A transverse abdominal incision was made and the ligaments connecting the superior and inferior portions of the liver were dissected. The gastric and splenic branches of the portal, as well as the hepatic artery, were ligated with 6–0 silk (Fine Science Tools inc, Foster City CA, USA). The bile duct was then partially dissected and cannulated with PE-10 tubing (Fisher Scientific). 0.1 U/g heparin was injected into the inferior vena cava through a 30G insulin syringe (Westnet, Canton MA, USA). 5 min later, the portal vein was cannulated with a 16G cannula (Westnet), and the liver was immediately flushed with 50 mL UW at approximately 10mL/min, either with or without 200 nM AP39. The remaining connective tissue was then dissected, and the liver was freed from the abdomen. The liver was immediately weighed, and subsequently either perfused for 6 h at 37 °C as described below (fresh control, $n = 4$), or flushed with UW with 200 nM AP39 (MedChemExpress, Monmouth Junction NJ, USA, $n = 6$) or vehicle (0.13% v/v dichloromethane, $n = 6$) and stored at 4 °C in the same respective solution for 3 days.

Machine perfusion

Livers were perfused on a homemade machine perfusion system as previously described²³. Briefly, a roller pump (Masterflex L/S, Vernon Hills IL, USA) circulated perfusate from a 500 mL basin using 16G in and outflow tubing (Masterflex). Before reaching the liver, the circuit entered a double-jacketed oxygenator (Radnoti, Covina CA, USA), followed by a bubble trap (Radnoti). The system was heated to 37 °C by a circulating water bath

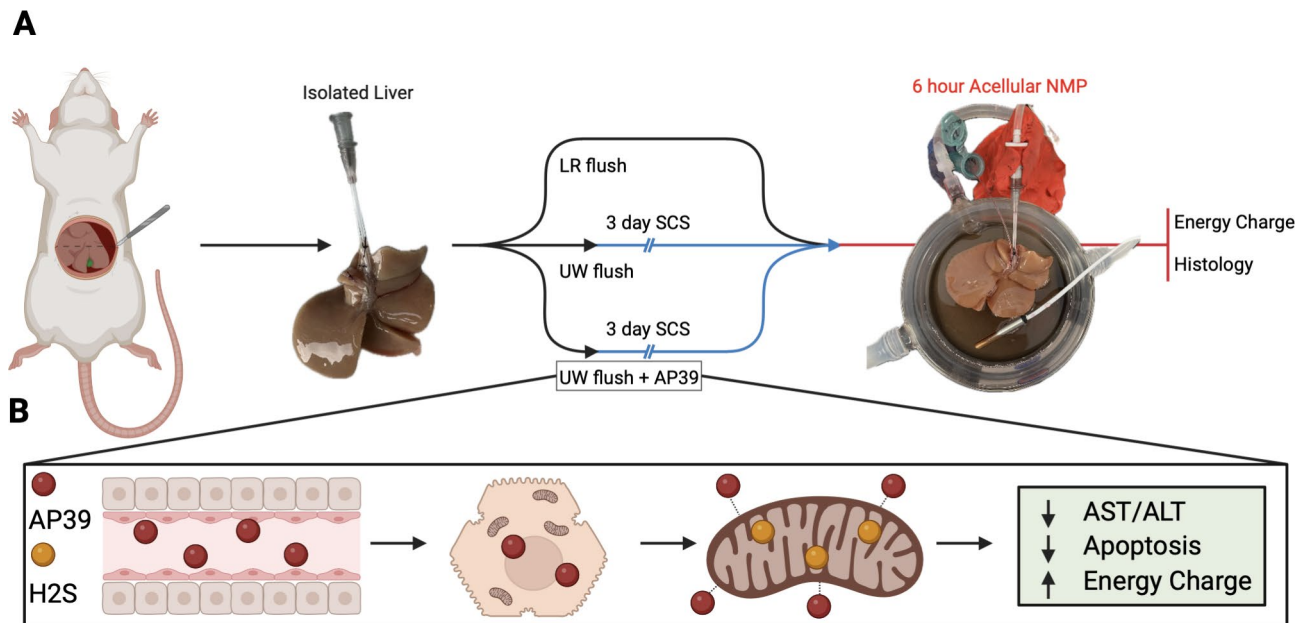


Fig. 1. Experimental outline and proposed AP39 mechanism: experimental schematic detailing the timeline of procurement and perfusion (a). Proposed mechanism by which AP39 enters the cell and donates H₂S directly to mitochondria (b).

(PolyScience, Niles IL, USA). Inflow perfusate oxygen concentration was maintained between 500 and 600 mmHg by a 21% O₂, 5% CO₂, balance N₂ tank (Airgas, Radnor PA, USA). The liver intravascular pressure was zeroed according to system pressure using a portable pressure monitor (Sciatica, London ON, Canada), continuously monitored throughout the perfusion. The liver was hand-flushed with 50 mL lactated ringers (Baxter, Deerfield IL, USA), and attached to the system at a flow of 5 mL/min. After a short (1–2 min) adjustment period, the flow was rapidly raised to 30 mL/min, maintaining a pressure below 11 mmHg. Outflow samples were collected from the suprahepatic IVC, every 30 min, and inflow samples were taken from a side port immediately before the arterial cannula perfusing the liver. Samples were analyzed using a Siemens Rapidpoint 500 (Siemens, Munich, Germany). Oxygen consumption was calculated according to the following equation: $OUR = (\text{inflow } O_2 - \text{outflow } O_2) * \text{flow rate} / \text{initial weight}$. Resistance was calculated according to the following equation: $R = \text{pressure} / \text{flow rate} / \text{initial weight}$. Pressure and flow were recorded every 15 min for the first 2 h, and every 30 min thereafter. At the end of perfusion, two biopsies were taken from the peripheral left lateral lobe; one of which was stored in 1% formalin, while the other was immediately snap-frozen in liquid nitrogen.

Perfusate composition

The perfusate was composed from a base of 500 mL William's Medium E (WE) (with sodium bicarbonate, without L-glutamine, with phenol red) (Sigma-Aldrich, St. Louis, MO, USA) into which, the following was added: 1% w/v bovine serum albumin (Sigma-Aldrich), 1% v/v sodium heparin (1,000 U/mL) (MGH Pharmacy), 100 uL insulin (MGH Pharmacy), 200 uL hydrocortisone (MGH Pharmacy), and 0.4% v/v penicillin-streptomycin (Thermo Fisher Scientific, Waltham MA, USA).

ALT and AST assay

AST and ALT levels were measured using a commercially available colorimetric activity assay (Cayman Chemicals, Ann Arbor MI, USA) according to the manufacturer's instructions and as previously published²⁴. Outflow perfusate from 1, 3, and 6 h was incubated with LDH enzyme, and the oxidation of NADH was measured over time according to the absorbance at 340 nm.

GLDH assay

GLDH activity was measured using a commercially available colorimetric activity assay (Abcam, Cambridge, United Kingdom) according to the manufacturer's instructions. Outflow perfusate from 1 to 6 h was incubated with glutamate, and the activity of GLDH was determined by the production of NADH over time according to the absorbance at 450 nm.

MDA assay

MDA concentration was measured using a commercially available colorimetric activity assay (Sigma-Aldrich, St. Louis MO, USA) according to the manufacturer's instructions. Protein was isolated from flash-frozen tissue taken at hour 6 and was homogenized with lysis buffer. Isolated protein was then incubated with TBA solution at 95 °C, after which absorbance was read at 532 nm.

Histological analysis

Histology samples were moved from formalin to 70% ethanol after 24 h. Sections were stained with hematoxylin and eosin (H&E) and terminal deoxynucleotidyl dUTP nick end labeling (TUNEL) as previously published^{25,26}. Slides were then imaged at 20X on a Nikon Eclipse E800. On H&E slides, liver sinusoidal endothelial cells (LSEC) sloughing and congestion of the portal vein were analyzed. TUNEL staining was quantified using the Weka trainable segmentation plugin in Fiji²⁷. Briefly, nuclei were classified as apoptotic if they were stained brown, or alive if they were stained purple. A probability map of live and dead cells was produced and particle count was applied to find the ratio of dead cells to live cells. All tissue processing was performed at the MGH Histology Molecular Pathology Core Facility (Boston, MA, USA).

Metabolite analysis

Metabolites were analyzed as previously described^{28,29}. Liver samples were crushed in liquid nitrogen, and metabolites were extracted using an established procedure³⁰. All mass spectrometry experiments were performed on a Triple TOF 6600 system (AB Sciex) hooked with a Shimadzu HPLC LC20AD (Shimadzu America) system. Compounds were separated on an analytical Luna NH₂ column 2 × 150 mm, 3 μm, 100 Å equipped with a 2.0 × 4 mm guard column (Phenomenex) using the following conditions: mobile phase A – 100% 5 mM ammonium acetate in water, adjusted to pH 9.9 with ammonium hydroxide; mobile phase B – 100% acetonitrile (ACN). Briefly, injection was performed at 20% A, followed immediately by a linear gradient to 100% A over 20 min, hold at 100% A for 4 min, drop to 20% A over 1 min and hold for 5 min at 20% A. The flow rate was set at 0.2 ml/min; column temperature was 25 °C; injection volume was 2 μl, and autosampler temperature was 4 °C, with a total runtime of 30 min including mobile phase equilibration. The mass spectrometer was set to acquire TOF MS spectrum followed by a dedicated product ion spectrum in high sensitivity mode for all nine metabolites of interest. This workflow is also referred to as MRMHR by the vendor. MS spectrum dwell time was 250 msec and each product ion spectrum was 100 msec. All mass spectrometry experiments were performed in positive electrospray ionization mode. The instrument was set to autocalibrate after acquisition of 5 samples. Briefly, autocalibration was performed by injecting 1 μl of a solution containing 0.5 μmolar AMP, 0.3 μmolar GSSG & 0.2 μmolar FAD. Ion source parameters were as follows: nebulizer gas (gas 1) was 50 psi, heater gas (gas 2) was 55 psi, source temperature 450 °C, ionspray voltage was 5500 V, mass range for each experiment 100–900 m/z. Once the mass spec data are recorded, MultiQuant 3.0.2 (AB Sciex) software was used for quantitation by generating chromatographic peak areas. Concentrations of metabolites in unknown

samples were determined from standard curves constructed for each metabolite in the MultiQuant software. An eight point standard curve was generated each time prior to running samples using a mixture of known concentrations of the metabolites. All compounds eluted between 13 and 22 min.

Lead acetate detection

H₂S production was quantified as previously published^{6,10}. Briefly, tissue powder was homogenized in passive lysis buffer (PLB E1941, Promega) and the protein concentration was determined using the ThermoFisher Pierce™ BCA Protein Assay Kit (Cat# 23227). In a 96-well plate covered with Whatmann paper soaked in 20 mM lead acetate, samples were diluted (80 µg of protein in 80 L of PBS) and combined with 20 L of reaction mix containing PBS, 1 mM Pyridoxal 5'-phosphate (PLP) (82870, Sigma), and 10 mM Cysteine (c7352, Sigma). The plate was then incubated in a dry incubator at 37 °C for 2–4 h until lead sulfide darkening of the paper occurred.

4-Hydroxynonenal immunostaining

4HNE (ab46545), Abcam, dilution 1:600 immunohistochemistry was performed on paraffin sections. After rehydration and antigen retrieval (TRIS-EDTA buffer, pH 9, 1 min in an electric pressure cooker autocuiseur Instant Pot duo 60 under high pressure), immunostaining was performed using the Rabbit specific HRP/DAB Detection IHC Detection Kit - Micro-polymer (ab236469, abcam) according to the manufacturer's instructions. Slides were further counterstained with hematoxylin.

Statistical analysis

Statistical analysis and graphing were performed using Prism 10 version 10.0.3 (GraphPad Software, San Diego CA, USA). All data was analyzed using ordinary one-way ANOVA followed by Tukey's multiple comparison test to compare groups and determine significance. Data was reported as means with standard deviation, differences were considered significant when $p < 0.05$.

Results

Addition of AP39 to UW improves liver perfusion following 3 days of static cold storage

First, we examined the effect of AP39 during SCS. Livers that were immediately harvested (fresh) or stored on ice for 3 days with (AP39) or without AP39 (SCS) were subsequently evaluated during a 6-hour ex-vivo normothermic perfusion, previously successfully employed to model transplantation³¹. After 3 days of SCS oxygen uptake was reduced compared to fresh livers. No difference was observed between livers stored with and without AP39. (Fresh 49.1 uL O₂/min* $g \pm 15.8$, SCS 33.9 uL O₂/min* $g \pm 13.1$, AP39 34.6 uL O₂/min* $g \pm 11.0$, $p = 0.9937$, Fig. 2a). Importantly, AP39 supplementation reduced vascular resistance (0.019 mmHg*min/L* $g \pm 0.012$, $p = 0.0457$) compared to SCS (0.027 mmHg*min/L* $g \pm 0.012$), and was comparable to fresh livers (0.012 mmHg*min/L* $g \pm 0.010$, $p < 0.0001$, Fig. 2b). No difference between the groups was observed in perfusion flow rate or edema at the end of perfusion (Figure S1a-c). Consistently, alanine aminotransferase (ALT, Fig. 2c) and aspartate aminotransferase (AST, Fig. 2d) liver transaminase reflecting cellular injury, were reduced in AP39-treated livers to levels similar to freshly perfused liver. No difference was observed in outflow pH, outflow lactate, or outflow glucose (Figure, S1d-f). The concentration of lead acetate showed no difference between groups (Figure S2). At 6 h post-reperfusion, perfusate glutamate dehydrogenase was significantly elevated in SCS (0.19 mU/mL ± 0.16) compared to fresh (0.03 mU/mL ± 0.01 , $p = 0.0432$) whereas no difference was observed between Fresh and AP39. No significant difference was observed between SCS and AP39 (0.07 mU/mL ± 0.04 , $p = 0.2961$, Figure S3). All perfusate electrolytes remained within normal range throughout perfusion (Figure S4).

AP39 improves hepatocellular function after static cold storage

Next we evaluated whether hepatocellular function was improved by AP39 after storage, and during ex-vivo normothermic ex-vivo perfusion. Bile production was similarly reduced in SCS (17.9 uL/g ± 18.3) and AP39 (39.9 uL/g ± 18.2 , $p = 0.5079$) compared to fresh (376.4 uL/g ± 52.2 , $p < 0.0001$ for both) livers (Fig. 3a). However, bile glucose was higher in SCS (95.3 mg/dL ± 40.8) compared to AP39 (70.2 mg/dL ± 36.7 , $p = 0.4832$) and fresh (20 mg/dL ± 0 , $p = 0.192$, Fig. 3b). Interestingly, when plotting bile production, we observed a clear separation between livers stored with or without AP39 (Fig. 3c). We previously demonstrated that graft ATP level correlates with viability^{32,33}. While ATP tended to be higher in the AP39-treated liver, the ratio of ATP: AMP as well as ATP: ADP was similar in all three groups (Fig. 3d, e). However, the energy charge, a calculation based on the ratio of AMP, ADP, and ATP, also used as a marker for graft viability, was higher in AP39 (0.55 ± 0.11) compared to SCS (0.28 ± 0.16 , $p = 0.0065$, Fig. 3f). No difference was observed between SCS and AP39 in other bioenergetic molecules (Figure S5).

AP39 reduces apoptosis and liver damage

After simulated transplant, AP39 improved sinusoidal endothelial structure, with reduced sloughing compared to SCS (Fig. 4a). Consistently, hepatocytes showed reduced architectural disruption and hepatocellular shrinkage, suggesting reduced hepatocellular stress (Fig. 4a). Similarly, 3 days of SCS resulted in a 2-fold increase in the number of apoptotic cells compared to AP39 (Fig. 5a SCS 20.7 ± 10.7 vs. AP39 10.7 ± 2.1 , $p < 0.0001$ (Fig. 5b) as assessed by TUNEL. No significant difference in 4HNE staining or MDA activity was observed, indicating no difference in lipid peroxidation (Figure S6).

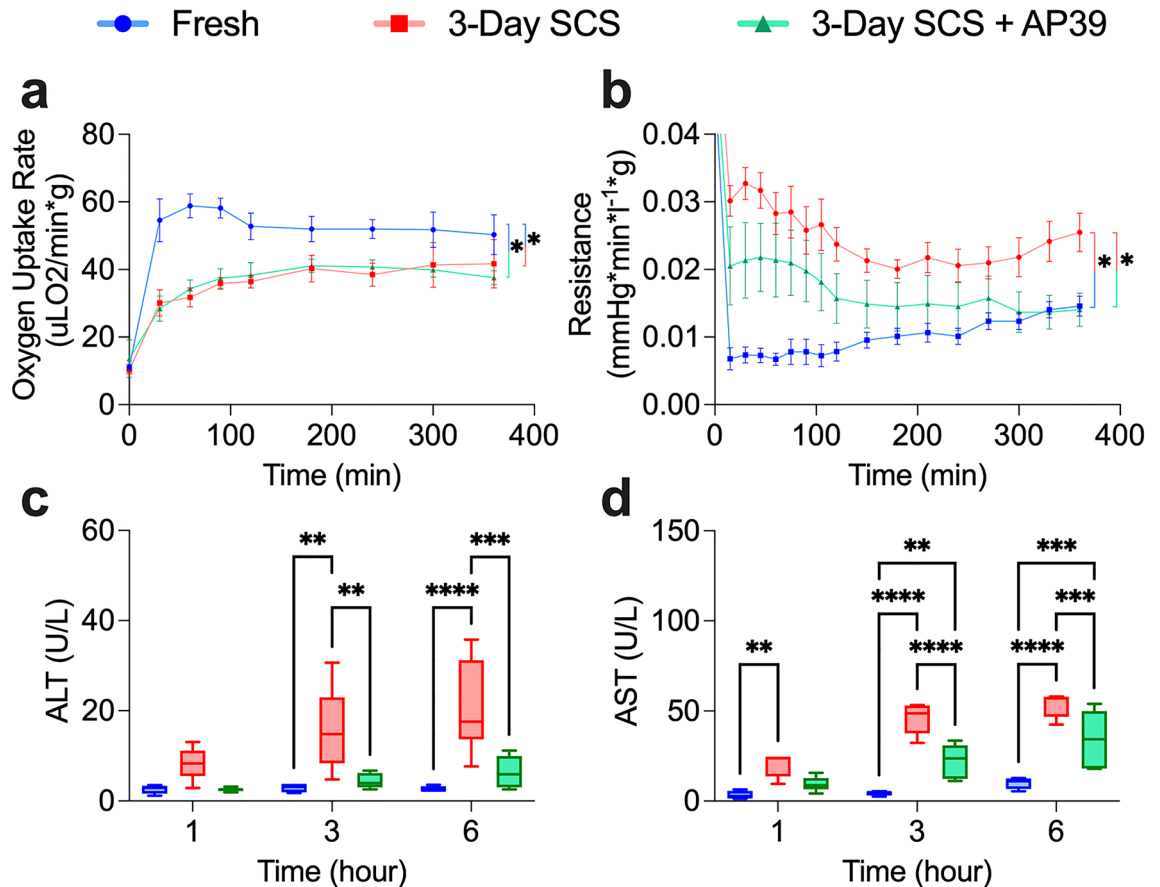


Fig. 2. Addition of AP39 to UW improves perfusion parameters following 3 days of static cold storage: comparison of perfusion metrics during acellular normothermic machine perfusion following 3 days of SCS. **(a)** Oxygen consumption was diminished in both SCS groups. **(b)** Resistance in SCS without AP39 was elevated compared to both fresh and SCS + AP39, while no difference was observed between fresh and SCS + AP39. **(c)** ALT and **(d)** AST were both elevated. No difference was seen between Fresh and SCS + AP39, although AST was elevated beyond 3 h. Asterisks denote statistical significance (ordinary one-way ANOVA with multiple comparisons test) * $0.01 < p < 0.05$; ** $0.001 < p < 0.01$; *** $0.0001 < p < 0.001$; **** $p < 0.0001$. Boxes, median and interquartile range. Whiskers, 5th – 95th percentile. Error bars of line graphs, mean \pm S.E.M.

Discussion

In this study, the addition of the slow-releasing, mitochondrial targeting H₂S donor AP39 to UW storage solution during SCS reduced post-reperfusion injury and improved cellular function in rat livers. While AP39 was shown to improve heart, kidney, and pancreas function following cold storage, this is the first study investigating its impact during SCS in a liver model^{19,34,35}.

The current clinical limitation for liver storage prior to transplantation is between 9 and 12 h, restricted by the persistence of metabolism at 4 °C, inexorable consumption of cellular energy stores, and ROS production during reperfusion³⁶. Surprisingly we observed that oxygen consumption was reduced in livers treated with AP39. Oxygen consumption is a measurement of oxygen extraction during perfusion, shown to correlate with transplant outcomes in rat models²⁰. Following cold storage, rat livers are known to exhibit reduced oxygen consumption, which is thought to reflect mitochondrial dysfunction^{26,37}. Similarly, H₂S transiently inhibits oxygen consumption in the absence of cellular injury and induces a suspended animation state via inhibition of oxidative phosphorylation at complex I and IV^{6,38–40}. No difference in endogenous H₂S production capacity was observed, indicating that exogenous H₂S generation by AP39 has no impact on this pathway. Consistently, with the benefit of transition inhibition of oxidative phosphorylation by H₂S, AP39 was also associated with a reduction in hepatic transaminase (ALT and AST), a surrogate of hepatocellular injury⁴¹. Additionally, apoptosis was reduced in AP39 treated livers, which might be associated with a reduction in the release of damage-associated molecular patterns following reperfusion⁴². A lack of GLDH elevation in AP39 livers indicates that the drug appears to reduce mitochondrial injury; however, further analysis is required to elucidate the protective mechanism. Interestingly, a slight, though non-significant reduction in lipid peroxidation was observed, indicating that the protective mechanism of AP39 after 3-days of storage may involve pathways outside of reactive oxygen species.

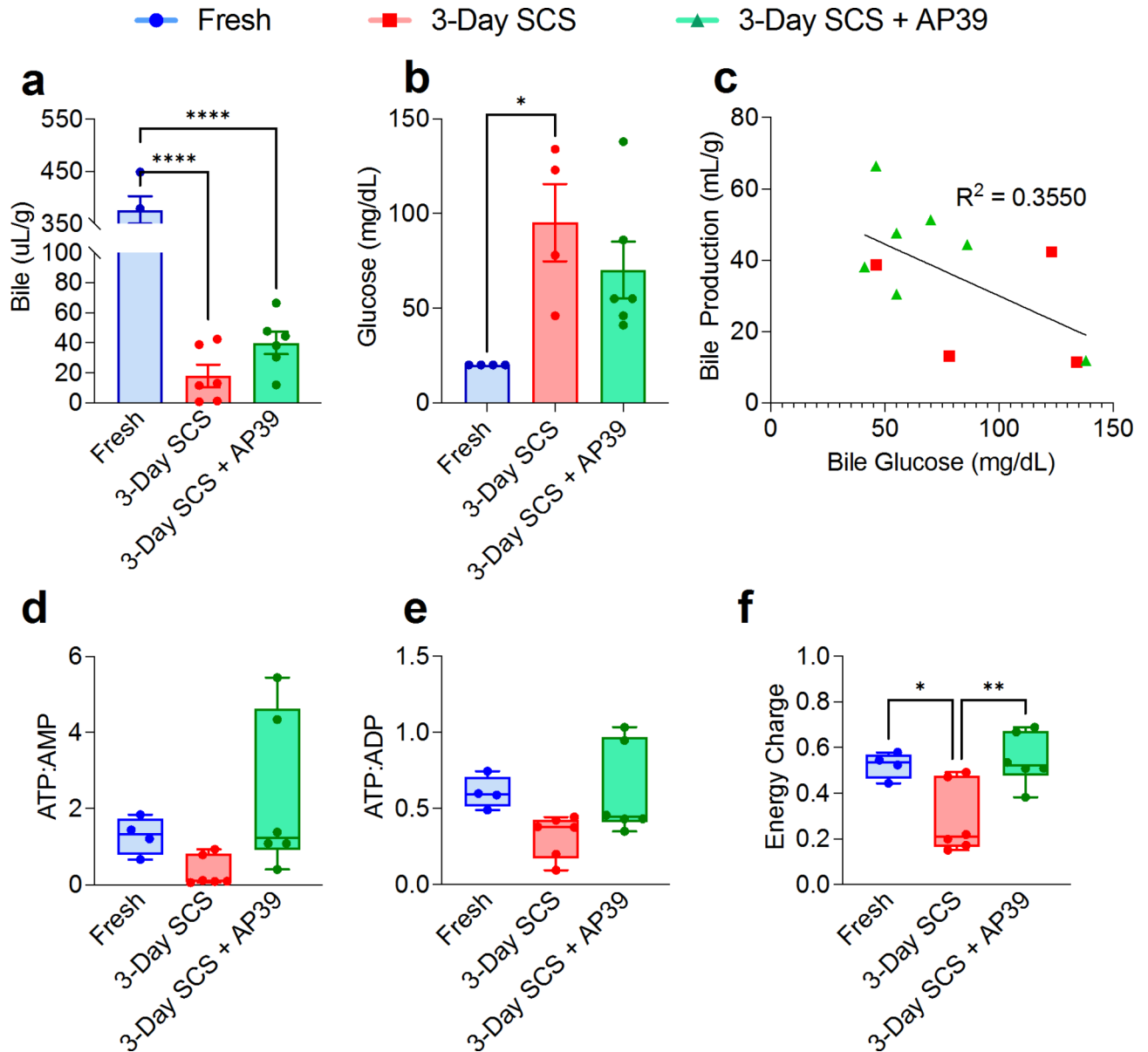


Fig. 3. Functional parameters show improved hepatocellular functionality when stored with AP39: bile was collected through the perfusions and, at the end of experiment, was measured. **(a)** Production was diminished in SCS livers, however, a slight increase was observed in SCS + AP39 compared to SCS. **(b)** When measured for metabolic parameters, bile glucose was elevated SCS compared to Fresh, while no elevation was observed between Fresh and SCS + AP39. **(c)** When plotting bile production against bile glucose, a weak correlation of $r^2 = 0.3550$ was observed, although this correlation is limited by the fact that several SCS livers did not produce enough bile for measurement. At the end of perfusion, biopsies were taken and snap frozen in liquid nitrogen, after which key metabolic parameters were measured using LC-MS. The ratio of **(d)** ATP: AMP and **(e)** ATP: ADP was not different between groups, however, the **(f)** energy charge was diminished in SCS compared to Fresh and SCS + AP39, while no difference was observed between these two groups. Asterisks denote statistical significance (ordinary one-way ANOVA with multiple comparisons test) * $0.01 < p < 0.05$; ** $0.001 < p < 0.01$; *** $0.0001 < p < 0.001$; **** $p < 0.0001$. Boxes, median and interquartile range. Whiskers, 5th – 95th percentile. Error bars of bar charts, mean \pm s.e.m.

Vascular resistance was improved in livers treated with AP39. Of interest, LSECs are highly susceptible to IR injury⁴³. In addition, AP39 was shown to promote vasorelaxation through modulation of NO-signaling; indicating that AP39 may directly improve LSEC outcome following reperfusion^{44,45}. H₂S has been shown to directly improve LSEC health during sepsis by reducing defenestration⁴⁶. LSEC sloughing is a common indicator of LSEC following reperfusion injury⁴⁷. Similarly, a reduction in LSEC sloughing was observed on H&E. Consistently, portal congestion is commonly observed when blood flow is impaired⁴⁸. Interestingly, a reduction in portal congestion was observed in livers stored with AP39⁴⁹.

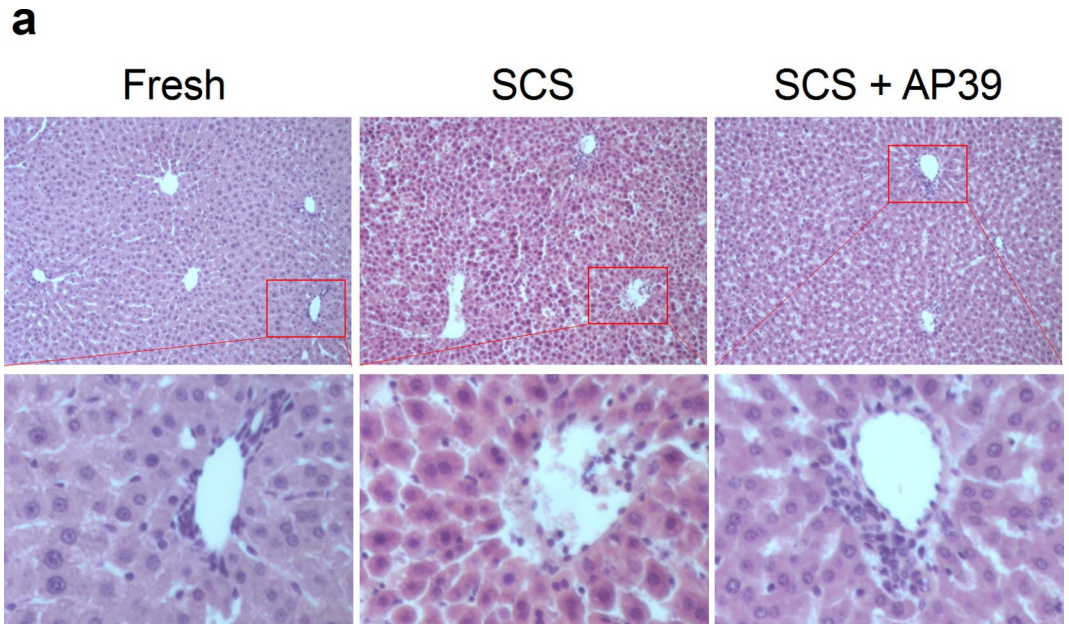


Fig. 4. Hematoxylin and eosin staining reveals improved liver microstructure when stored with AP39: at the end of perfusion, biopsies were taken and formalin fixed, after which they were paraffin embedded and stained with (a) hematoxylin and eosin. Microscopic analysis reveals improved cellular morphology in SCS compared to SCS + AP39, with reduced cellular shrinking. Additionally, portal congestion was decreased in SCS + AP39, and endothelial structure was better maintained, showing a similar vascular pattern to Fresh. Asterisks denote statistical significance (ordinary one-way ANOVA with multiple comparisons test) $*0.01 < p < 0.05$; $**0.001 < p < 0.01$; $***0.0001 < p < 0.001$; $****p < 0.0001$. Boxes, median and interquartile range. Whiskers, 5th – 95th percentile.

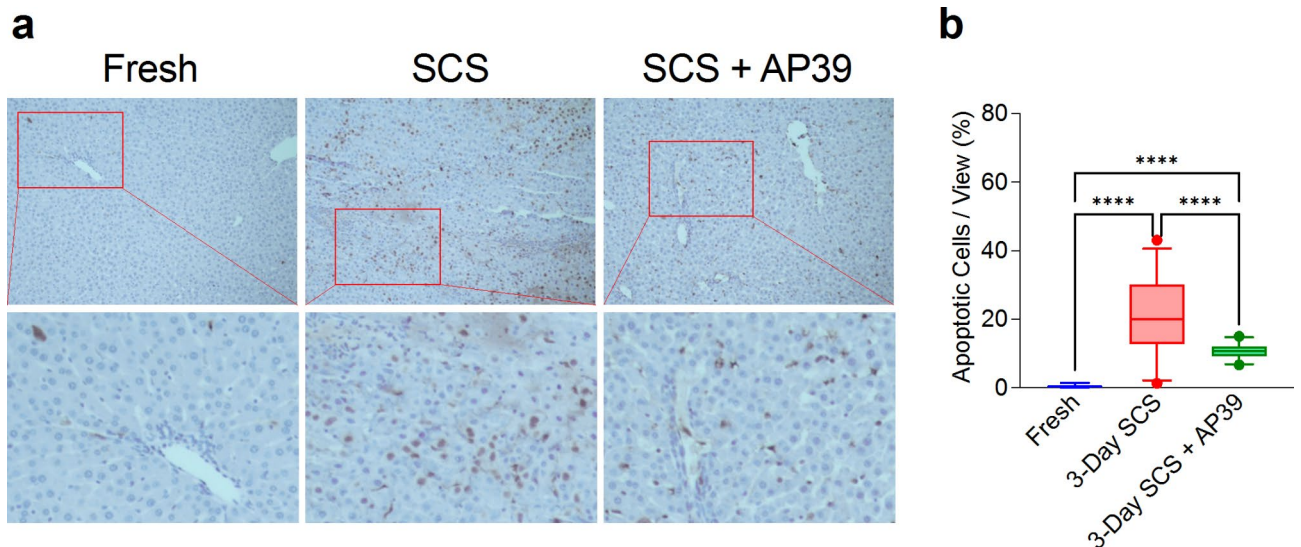


Fig. 5. TUNEL staining shows decreased apoptosis in livers stored with AP39: formalin fixed samples were also stained with terminal deoxynucleotidyl transferase (TUNEL) stain, revealing double-strand DNA breaks, a marker of apoptosis, in brown. (a) SCS + AP39 showed a marked reduction in TUNEL positive staining compared to SCS, although still elevated when compared to Fresh. (b) Following quantification, SCS without AP39 showed a greatly increased percentage of apoptotic positive cells compared to SCS + AP39. Asterisks denote statistical significance (ordinary one-way ANOVA with multiple comparisons test) $*0.01 < p < 0.05$; $**0.001 < p < 0.01$; $***0.0001 < p < 0.001$; $****p < 0.0001$. Boxes, median and interquartile range. Whiskers, 5th – 95th percentile.

Compared to fresh livers, SCS resulted in a reduction in bile production. Although not significant, this was improved by AP39. Of interest, the relationship between bile production and bile glucose demonstrated 2 distinct clusters between livers stored with and without AP39. Potentially, a larger difference and stronger clustering may have been observed if bile glucose were able to be measured for all livers stored without AP39 (no bile production). Consistent with the protective role of AP39, bile production, and quality were associated with both post-transplant liver health and functionality^{50,51}. Additionally, reduction in bile glucose and bile volume during normothermic machine perfusion was previously associated with liver viability⁵².

While the direct ratio of ATP: ADP and ATP: AMP was similar in livers stored with AP39, tissue energy charge, previously shown by our team to be associated with transplant outcome³³, was improved by AP39. Consistently, H₂S is shown to improve post-reperfusion energy stores in rat hearts following warm ischemia^{32,53}. Despite improvements in energy charge, a reduction in NADH: NAD⁺ ratio was observed in livers stored with AP39. NADH has been shown to accumulate during the storage of rat livers as the electron transport chain is compromised, with reduced complex I function⁵⁴. Decreased NAD⁺ levels, when combined with improved energy charge, indicate that following reperfusion, mitochondria with AP39 show improved ATP production⁵⁵.

Limitations are acknowledged. First the use of an acellular media strictly limits the IR injury caused by immune response such as neutrophil activation and subsequent parenchymal migration, inducing degranulation and protease activity⁵⁶. Second, despite similarities in microarchitecture between rodent and human livers, several key differences are present such as a reduction in connective tissue in rodent livers, increased perfusate delivery through the portal vein as compared to human livers, and a different surface area to volume ratio⁵⁷. Additionally, the lack of transplantation, and relatively short perfusion period limits our understanding regarding the long-term impact of AP39 supplementation. Future studies should perform further work into elucidating the mechanism by which AP39 ameliorates ischemia-reperfusion-injury in larger human organs and in the context of transplantation.

Altogether this study demonstrates that AP39 supplementation in UW during SCS reduced hepatocellular injury during preservation, improving graft function during simulated transplantation. These results provide the basis for next-generation organ preservation solutions and should be translatable to human livers.

Data availability

Data is provided within the manuscript and supplementary information. Additional data are available from the corresponding author by reasonable request.

Received: 28 May 2024; Accepted: 1 January 2025

Published online: 10 January 2025

References

- Kwong, A. J. et al. OPTN/SRTR 2021 annual data report: Liver. *Am J Transplant* **23**(2 Suppl 1), S178–S263 (2023).
- Giwa, S. et al. The promise of organ and tissue preservation to transform medicine. *Nat. Biotechnol.* **35**(6), 530–542. <https://doi.org/10.1038/nbt.3889> (2017).
- Haugen, C. E. et al. Assessment of trends in transplantation of liver grafts from older donors and outcomes in recipients of liver grafts from older donors 2003–2016. *JAMA Surg.* **154**(5), 441–449. <https://doi.org/10.1001/jamasurg.2018.5568> (2019).
- McFarlane, L., Nelson, P., Dugbartey, G. J. & Sener, A. Pre-treatment of transplant donors with hydrogen sulfide to protect against warm and cold ischemia-reperfusion injury in kidney and other transplantable solid organs. *Int. J. Mol. Sci.* **24**(4) (2023).
- Polhemus, D. J. & Lefer, D. J. Emergence of hydrogen sulfide as an endogenous gaseous signaling molecule in cardiovascular disease. *Circ. Res.* **114**(4), 730–737 (2014).
- Longchamp, A. et al. Amino Acid Restriction Triggers Angiogenesis via GCN2/ATF4 Regulation of VEGF and H(2)S Production. *J Cell* **173**(1), 117–129 e14 (2018).
- Modis, K., Coletta, C., Erdelyi, K., Papapetropoulos, A. & Szabo, C. Intramitochondrial hydrogen sulfide production by 3-mercaptopyruvate sulfurtransferase maintains mitochondrial electron flow and supports cellular bioenergetics. *FASEB J.* **27**(2), 601–611 (2013).
- Gemici, B. & Wallace, J. L. Anti-inflammatory and cytoprotective properties of hydrogen sulfide. *Methods Enzymol.* **555**, 169–193 (2015).
- Berkane, Y. et al. Supercooling: a promising technique for prolonged preservation in solid organ transplantation, and early perspectives in vascularized composite allografts. *Front. Transp.* **2** (2023).
- Hine, C. et al. Endogenous hydrogen sulfide production is essential for dietary restriction benefits. *Cell* **160**(1–2), 132–144 (2015).
- Hashmi, S. F. et al. Hydrogen sulphide treatment prevents renal ischemia-reperfusion injury by inhibiting the expression of ICAM-1 and NF-κB concentration in normotensive and hypertensive rats. *Biomolecules* **11**(10) (2021).
- Zhang, M. Y. et al. Sodium thiosulfate-supplemented UW solution protects renal grafts against prolonged cold ischemia-reperfusion injury in a murine model of syngeneic kidney transplantation. *Biomed. Pharmacother.* **145**, 112435 (2022).
- Kang, K. et al. Role of hydrogen sulfide in hepatic ischemia-reperfusion-induced injury in rats. *Liver Transpl.* **15**(10), 1306–1314 (2009).
- Lee, Z. W. et al. The slow-releasing hydrogen sulfide donor, GYY4137, exhibits novel anti-cancer effects in vitro and in vivo. *PLoS One* **6**(6), e21077 (2011).
- Szczesny, B. et al. AP39, a novel mitochondria-targeted hydrogen sulfide donor, stimulates cellular bioenergetics, exerts cytoprotective effects and protects against the loss of mitochondrial DNA integrity in oxidatively stressed endothelial cells in vitro. *Nitric Oxide* **41**, 120–130 (2014).
- Gero, D. et al. The novel mitochondria-targeted hydrogen sulfide (H(2)S) donors AP123 and AP39 protect against hyperglycemic injury in microvascular endothelial cells in vitro. *Pharmacol. Res.* **113**(Pt A), 186–198 (2016).
- Lobb, I. et al. Hydrogen sulfide protects renal grafts against prolonged cold ischemia-reperfusion injury via specific mitochondrial actions. *Am. J. Transpl.* **17**(2), 341–352 (2017).
- Juriasingani, S. et al. Evaluating the effects of subnormothermic perfusion with AP39 in a novel blood-free model of ex vivo kidney preservation and reperfusion. *Int. J. Mol. Sci.* **22**(13) (2021).
- Zhu, C. et al. Supplementing preservation solution with mitochondria-targeted H(2) S donor AP39 protects cardiac grafts from prolonged cold ischemia-reperfusion injury in heart transplantation. *Am. J. Transpl.* **19**(11), 3139–3148 (2019).
- Berendsen, T. A. et al. Supercooling enables long-term transplantation survival following 4 days of liver preservation. *Nat. Med.* **20**(7), 790–793 (2014).

21. Jain, R. et al. Real-time monitoring of mitochondrial oxygenation during machine perfusion using resonance Raman spectroscopy predicts organ function. *Sci. Rep.* **14**(1), 7328 (2024).
22. Bruinsma, B. G., Berendsen, T. A., Izamis, M. L., Yarmush, M. L. & Uygun, K. Determination and extension of the limits to static cold storage using subnormothermic machine perfusion. *Int. J. Artif. Organs* **36**(11), 775–780 (2013).
23. Tessier, S. N. et al. Partial freezing of rat livers extends preservation time by 5-fold. *Nat Commun* **13**(1), 4008 (2022).
24. Yang, R. Z. et al. Alanine aminotransferase isoenzymes: Molecular cloning and quantitative analysis of tissue expression in rats and serum elevation in liver toxicity. *Hepatology* **49**(2), 598–607 (2009).
25. Kyrylkova, K., Kyryachenko, S., Leid, M. & Kioussi, C. Detection of apoptosis by TUNEL assay. *Methods Mol. Biol.* **887**, 41–47 (2012).
26. Haque, O. et al. The effect of blood cells retained in rat livers during static cold storage on viability outcomes during normothermic machine perfusion. *Sci. Rep.* **11**(1), 23128 (2021).
27. Schindelin, J. et al. Fiji: An open-source platform for biological-image analysis. *Nat. Methods* **9**(7), 676–682 (2012).
28. Agius, T. et al. Subnormothermic ex vivo porcine kidney perfusion improves energy metabolism: Analysis using (31)P magnetic resonance spectroscopic imaging. *Transp. Direct* **8**(10), e1354 (2022).
29. Raigani, S. et al. Metabolic and lipidomic profiling of steatotic human livers during ex situ normothermic machine perfusion guides resuscitation strategies. *PLoS ONE* **15**(1), e0228011 (2020).
30. Yuan, M., Breikopf, S. B., Yang, X. & Asara, J. M. A positive/negative ion-switching, targeted mass spectrometry-based metabolomics platform for bodily fluids, cells, and fresh and fixed tissue. *Nat. Protoc.* **7**(5), 872–881 (2012).
31. Mojoudi, M. et al. Anti-apoptotic treatment of warm ischemic male rat livers in machine perfusion improves symptoms of ischemia-reperfusion injury. *Heliyon* **10**(8), e29519 (2024).
32. Agius, T. et al. Sodium hydrosulfide treatment during porcine kidney ex vivo perfusion and transplantation. *Transpl. Direct* **9**(11), e1508 (2023).
33. Bruinsma, B. G. et al. Metabolic profiling during ex vivo machine perfusion of the human liver. *Sci. Rep.* **6**, 22415 (2016).
34. Ahmad, A. et al. AP39, a mitochondrially targeted hydrogen sulfide donor, exerts protective effects in renal epithelial cells subjected to oxidative stress in vitro and in acute renal injury in vivo. *Shock* **45**(1), 88–97 (2016).
35. Nishime, K. et al. Preservation of pancreas in the University of Wisconsin solution supplemented with AP39 reduces reactive oxygen species production and improves islet graft function. *Am. J. Transpl.* **21**(8), 2698–2708 (2021).
36. Porte, R. J. et al. Long-term graft survival after liver transplantation in the UW era: Late effects of cold ischemia and primary dysfunction. European Multicentre Study Group. *Transpl. Int.* **11**(Suppl 1), S164–S167 (1998).
37. Zhang, H. et al. The role of mitochondria in liver ischemia-reperfusion injury: From aspects of mitochondrial oxidative stress, mitochondrial fission, mitochondrial membrane permeable transport pore formation, mitophagy, and mitochondria-related protective measures. *Oxid. Med. Cell Longev.* **2021**, 6670579 (2021).
38. Paul, B. D., Snyder, S. H. & Kashfi, K. Effects of hydrogen sulfide on mitochondrial function and cellular bioenergetics. *Redox Biol.* **38**, 101772 (2021).
39. Blackstone, E., Morrison, M. & Roth, M. B. H₂S induces a suspended animation-like state in mice. *Science* **308**(5721), 518 (2005).
40. Maassen, H. et al. Hydrogen sulphide-induced hypometabolism in human-sized porcine kidneys. *PLoS One* **14**(11), e0225152 (2019).
41. Siddiqui, M. B. et al. Range of normal serum aminotransferase levels in liver transplant recipients. *Transpl. Proc.* **51**(6), 1895–1901 (2019).
42. Liu, H. & Man, K. New insights in mechanisms and therapeutics for short- and long-term impacts of hepatic ischemia reperfusion injury post liver transplantation. *Int. J. Mol. Sci.* **22**(15) (2021).
43. Russo, L. et al. Addition of simvastatin to cold storage solution prevents endothelial dysfunction in explanted rat livers. *Hepatology* **55**(3), 921–930 (2012).
44. Shah, V. et al. Liver sinusoidal endothelial cells are responsible for nitric oxide modulation of resistance in the hepatic sinusoids. *J. Clin. Investig.* **100**(11), 2923–2930 (1997).
45. da Costa Marques, L. A. et al. Vasorelaxant activity of AP39, a mitochondria-targeted H₂S donor, on mouse mesenteric artery rings in vitro. *Biomolecules* **12**(2) (2022).
46. Gaddam, R. R. et al. Cystathionine-Gamma-lyase-derived hydrogen sulfide-regulated substance P modulates liver sieve fenestrations in caecal ligation and puncture-induced sepsis. *Int. J. Mol. Sci.* **20**(13) (2019).
47. Fan, C. Q. & Crawford, J. M. Sinusoidal obstruction syndrome (hepatic veno-occlusive disease). *J. Clin. Exp. Hepatol.* **4**(4), 332–346 (2014).
48. Hilscher, M. & Sanchez, W. Congestive hepatopathy. *Clin. Liver Dis. (Hoboken)* **8**(3), 68–71 (2016).
49. de Vries, R. J. et al. Cell release during perfusion reflects cold ischemic injury in rat livers. *Sci. Rep.* **10**(1), 1102 (2020).
50. Kamiike, W. et al. Adenine nucleotide metabolism and its relation to organ viability in human liver transplantation. *Transplantation* **45**(1), 138–143 (1988).
51. Matton, A. P. M. et al. Biliary bicarbonate, pH, and glucose are suitable biomarkers of biliary viability during ex situ normothermic machine perfusion of human donor livers. *Transplantation* **103**(7), 1405–1413 (2019).
52. Thorne, A. M. et al. Bile proteome reveals biliary regeneration during normothermic preservation of human donor livers. *Nat. Commun.* **14**(1), 7880 (2023).
53. Bliksoen, M., Kaljusto, M. L., Vaage, J. & Stenslokken, K. O. Effects of hydrogen sulphide on ischaemia-reperfusion injury and ischaemic preconditioning in the isolated, perfused rat heart. *Eur. J. Cardiothorac. Surg.* **34**(2), 344–349 (2008).
54. Thorniley, M. S., Simpkin, S., Fuller, B., Jenabzadeh, M. Z. & Green, C. J. Monitoring of surface mitochondrial NADH levels as an indication of ischemia during liver isograft transplantation. *Hepatology* **21**(6), 1602–1609 (1995).
55. Schlegel, A. et al. Hypothermic oxygenated perfusion protects from mitochondrial injury before liver transplantation. *EBioMedicine* **60**, 103014 (2020).
56. Oliveira, T. H. C., Marques, P. E., Proost, P. & Teixeira, M. M. M. Neutrophils: A cornerstone of liver ischemia and reperfusion injury. *Lab. Investig.* **98**(1), 51–62 (2018).
57. Kruepunga, N., Hakvoort, T. B. M., Hikspoors, J., Kohler, S. E. & Lamers, W. H. Anatomy of rodent and human livers: What are the differences?. *Biochim. Biophys. Acta Mol. Basis Dis.* **1865**(5), 869–878 (2019).

Acknowledgements

This material is partially based upon work supported by the National Science Foundation under Grant No. EEC 1941543. Support from the US National Institutes of Health is gratefully acknowledged for the following awards: R01DK114506, R01DK096075, R01EB028782.

Author contributions

M.T, A.L, and K.U developed and outlined the study. S.H, A.T, M.H, and C.T performed the perfusions. M.T, M.M, and O.O performed the liver procurements. M.T, A.L performed perfusate and tissue analysis. M.T, S.H, and A.L performed the statistical analysis. M.T and A.L wrote the manuscript. M.T, J.M, H.Y, A.L, and K.U

participated in the critical revision of the manuscript. All authors contributed to the final preparation of the manuscript.

Declarations

Competing interests

The authors declare the following financial interests/personal relationships which may be considered as potential competing interests: Korkut Uygun reports financial support was provided by Massachusetts General Hospital. Korkut Uygun reports a relationship with National Institutes of Health that includes: funding grants. Some authors declare competing interests. Drs. Uygun and Yeh have patent applications relevant to this study. Dr. Uygun, has a financial interest in and serves on the Scientific Advisory Board for Sylvatica Biotech Inc., a company focused on developing high subzero organ preservation technology. Competing interests for MGH investigators are managed by the MGH and MGB in accordance with their conflict-of-interest policies. If there are other authors, they declare that they have no known competing financial interests or personal relationships that could have appeared to influence the work reported in this paper.

Additional information

Supplementary Information The online version contains supplementary material available at <https://doi.org/10.1038/s41598-025-85302-w>.

Correspondence and requests for materials should be addressed to K.U. or A.L.

Reprints and permissions information is available at www.nature.com/reprints.

Publisher's note Springer Nature remains neutral with regard to jurisdictional claims in published maps and institutional affiliations.

Open Access This article is licensed under a Creative Commons Attribution-NonCommercial-NoDerivatives 4.0 International License, which permits any non-commercial use, sharing, distribution and reproduction in any medium or format, as long as you give appropriate credit to the original author(s) and the source, provide a link to the Creative Commons licence, and indicate if you modified the licensed material. You do not have permission under this licence to share adapted material derived from this article or parts of it. The images or other third party material in this article are included in the article's Creative Commons licence, unless indicated otherwise in a credit line to the material. If material is not included in the article's Creative Commons licence and your intended use is not permitted by statutory regulation or exceeds the permitted use, you will need to obtain permission directly from the copyright holder. To view a copy of this licence, visit <http://creativecommons.org/licenses/by-nc-nd/4.0/>.

© The Author(s) 2025